CAGS2 Exchange Report

Guodong Yang[1], Aleks D. Atrens[2], Yilian Li[1], Hal Gurgenci[2]
[1]China University of Geosciences, Wuhan, 430074, China
[2]Queensland Geothermal Energy Centre of Excellence, The University of Queensland, Brisbane, 4072, Australia

Summary

This report outlines concepts related to the utilisation of injected CO_2 to promote production of thermal brines in the Jianghan Basin, China, thereby improving productivity of brine producing wells and potential for geothermal utilisation of heat contained in the brine. It firstly reviews the literature available on the utilisation of CO_2 in geothermal systems. It secondly describes the progress that has been achieved in the area of CO_2-geothermal by the Queensland Geothermal Energy Centre of Excellence. Finally, it discusses the development of a mass balance model of CO_2 injection into a brine filled reservoir. This mass balance model provides a basis for understanding the time scales for compositional changes within such a system, depending on variation of production flows of brine, input flows of CO_2, and general subsurface fluid flows. It can provide a foundation for future integrated models which combine a mass balance model – providing a link between fluid flows, reservoir volume, and pressure – and reservoir flow models, which predict the specific flow behaviour of individual injection or production wells as a function of reservoir pressure, composition, field layout, and time.

1. Research review on CO_2-EGS

Due to rapid economic development, energy demand is rapidly increasing. However, current primary energy sources – coal, oil, natural gas, and other fossil fuels – are non-renewable and potential threats to the global climate (Hameed, Cess et al. 1980, de Coninck, Meyer et al. 2005, Jones, Jones et al. 2005). It is urgent to find an alternative energy which is low-carbon, renewable and economical. Geothermal energy resources are an option which meets these criteria. The traditional approach for geothermal systems is to use water as the heat extraction fluid (André, Rabemanana et al. 2006, Lund, Bjelm et al. 2008, Zimmermann, Moeck et al. 2010), and engineered or enhanced geothermal systems have also operated in that manner. Using CO_2 instead of water as the heat extraction fluid to operate enhanced geothermal systems (EGS) is a recent concept, originally proposed by Brown (2000) (Brown 2000). As noted by Brown, CO_2 has attractive properties as a heat extraction and working fluid in EGS, and it could provide storage of greenhouse gases as an extra benefit. Table 1 shows a brief comparison of CO_2 and water for use as operating fluids in EGS; properties considered favourable are italicized (Pruess 2008).

Table 1 Comparing CO_2 and water as heat transmission fluid for EGS (from Pruess, 2008)

Fluid property	CO_2	Water
Chemistry	*Not an ionic solvent; poor solvent for rock minerals*	Powerful solvent for rock minerals: lots of potential for dissolution and precipitation
Fluid circulation in wellbores	*Large compressibility and expansivity*	small compressibility, moderate expansivity
	=> *More buoyancy, lower parasitic power consumption to maintain circulation*	=> Less buoyancy; substantial power requirements for pumps to keep fluids circulating
Ease of flow in reservoir	*Lower viscosity,* lower density	Higher viscosity, *higher density*
Heat transmission	Smaller specific heat	*Larger specific heat*
Fluid losses	*May earn credits for storing greenhouse gases*	Costly, obstacle to reservoir development

Favourable properties are italicized.

The use of CO_2 as the geothermal heat exchange fluid was further investigated by (Pruess 2006, Pruess 2008, Atrens, Gurgenci et al. 2009, Atrens, Gurgenci et al. 2010, Fard, Hooman et al. 2010, Spycher and Pruess 2010, Zimmermann, Moeck et al. 2010, Borgia, Pruess et al. 2012). Those studies mainly focus on the technical principles of CO_2-EGS, simulation and experimental research, system design and economic potential assessment.

Ueda et al. point out that a CO_2-based EGS is expected to comprise three reservoir zones (Ueda, Kato et al. 2005):

- Zone 1: The inner zone or "core" of the reservoir, from which all water has been removed by dissolution into the flowing CO_2 stream, so that the fluid consists of a single supercritical CO_2 phase. This is the main volume from which thermal energy is extracted by the flowing CO_2.
- Zone 2: This intermediate region surrounding the inner zone contains a two-phase mixture of CO_2 and aqueous fluid.
- Zone 3: The outermost region affected by EGS activities. The fluid is a single aqueous phase with dissolved and chemically active CO_2.

Process behaviour and issues are expected to be quite different in the three zones.

An initial quantitative exploration of the heat extraction and mass flow behaviour of CO_2-based EGS was reported in Pruess (2006) (Pruess 2006). The simulation studies indicate that it could be up to 50% more efficient to use CO_2 instead of water for geothermal energy development. Spycher et al. argue that there is a significant change in phase partitioning behaviour between water phase and supercritical CO_2 phase in the typical temperature and pressure conditions of CO_2-EGS. It is critical to establish a phase partitioning model in CO_2 and water solution mixtures over the entire range of temperature and pressure conditions to simulate multiphase flow and reactive solute transport processes of CO_2-EGS accurately (Spycher and Pruess 2010).

A number of numerical and laboratory works of CO_2-based EGS system have been examined over the past years. Rosenbauer et al. (Rosenbauer, Koksalan et al. 2005), Xu et al. (Xu 2008, Xu 2010), Xu and Pruess (Xu 2010), Wan et al. (Wan 2011), and Apps and Pruess (Apps 2011) carried out one- and two-dimensional thermo-hydrological-chemical (THC) simulations in order to assess the feasibility of using CO_2 as an operating fluid and accelerant for EGS, to evaluate the dissolution and precipitation reactions which could affect reservoir properties, and to understand the tradeoffs between power generation and CO_2 sequestration in mineral phases. Magliocco et al. (Magliocco 2011) performed laboratory experiments to study heat extraction from porous media by using CO_2.

Majorowicz et al. (Majorowicz and Grasby 2010) assessed the cost of CO_2-EGS system, and gave an evaluation of CO_2 reduction through conversion from coal and/or natural gas (NG) generation to EGS. Furthermore, they examined the Enhanced Geothermal Systems (EGS) potential for thermal and electrical power supply for communities in Canada in areas of previously defined high heat flow.

2. QGECE's research achievements on CO_2-EGS

The Queensland Geothermal Energy Centre of Excellence has been investigating the feasibility of a CO_2 geothermosiphon. Atrens et al.(Atrens, Gurgenci et al. 2009) modelled the performance and design of a hypothetical CO_2 thermosiphon, compared to a traditional water-based heat extraction system, as shown in Fig.1. The CO_2 geothermosiphon consists of an injection and a production well, the geothermal reservoir, a turbine, and a cooling system. Their results indicated that CO_2 and water-based EGS would generate similar amounts of electricity under ideal conditions (no frictional pressure losses in the wellbores, and a constant reservoir cross-section). More specifically, CO_2 geothermosiphon could produce 17 MWe of electricity when 80 MWth heat was extracted, while the power generation was estimated to be close to 18 MWe for an identical water-based system. In a subsequent study, Atrens et al. (Atrens, Gurgenci et al. 2010) extended the analysis of CO_2 geothermosiphon to include wellbore frictional pressure drop. The study showed that, compared to traditional water-based systems, while the reservoir pressure drop for a CO_2 geothermosiphon is lower, the wellbore frictional losses, especially those of the production well, are higher.

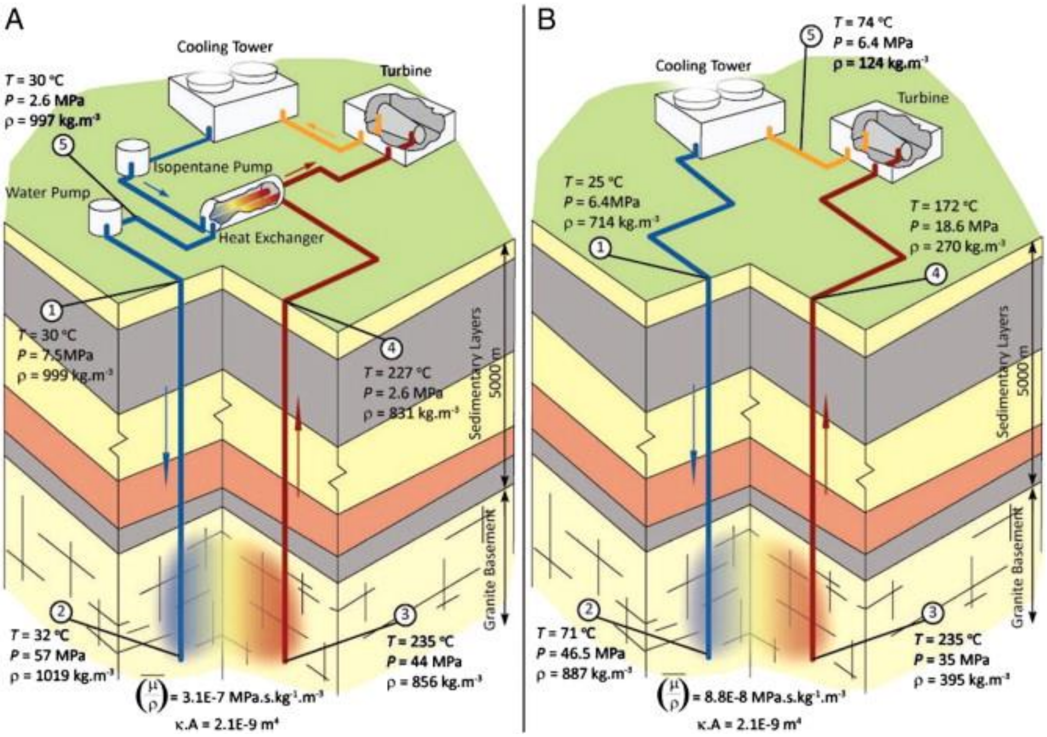

Fig.1. Geothermal plant design. A. water-based system. B. CO_2 geothermosiphon design (from A. D. Atrens, 2009)

Based on the previous work, Atrens et al. (Atrens, Gurgenci et al. 2011) explored the economics of the CO_2-based EGS technology for an optimized power plant design and best-available cost estimation data (Fig.2). They demonstrated that:

- Turbine exhaust to sub-injection pressures followed by recompression is economically favourable;
- Near-optimum turbine exhaust pressure can be estimated directly from surface temperature;
- Identifying that the achievable cooling temperature is an important economic site consideration alongside resource temperature; and
- They concluded that if fluid losses occur, the economic viability of the concept depends strongly on the price associated with CO_2.

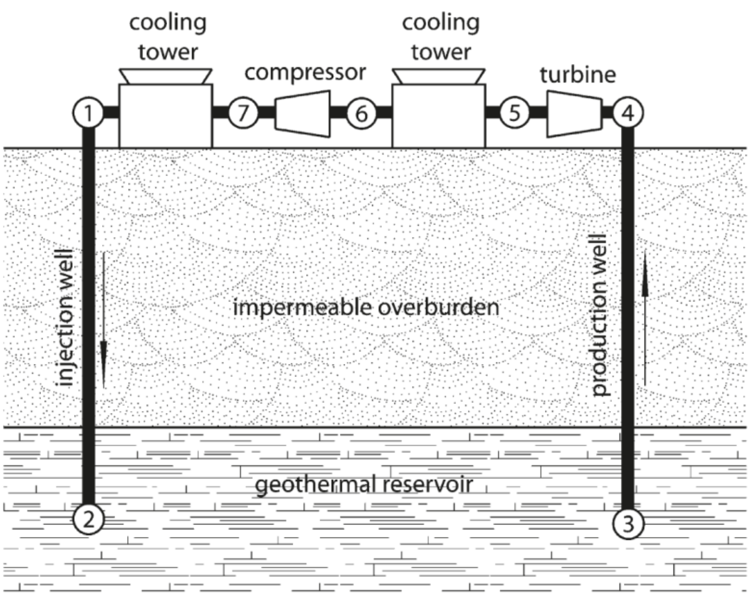

Fig.2. Conceptual diagram of the system (from A. D. Atrens)

Haghshenas et al. (Haghshenas Fard, Hooman et al. 2010) presented a detailed numerical simulation of the supercritical CO_2 geothermosiphon, and provided a criterion for assessing the significance of the frictional losses. Based on their numerical results and theoretical analysis of the problem, a rough and ready estimate for the overall heat transfer coefficient of the reservoir is presented as a function of fluid thermophysical properties, the injection mass flow rate, and the fracture wetted periphery.

The above research work provides a theoretical basis for site selection and design of CO_2-based geothermal power plant in the future. However, there are still complexity and uncertainty for CO_2-EGS to advance the concept from theory to practical application. Further research on these topics has to be conducted in the future.

3. Design of Coupling Brine Extraction and Energy Production from Geopressured-Geothermal Aquifers using CO_2 in Jianghan Basin, China

3.1 Introduction

The storage of CO_2 in deep saline aquifers as well as the extraction of brine (Buscheck, Sun et al. 2011) and geothermal energy (heat) from geothermal reservoirs have been studied independently in the past. However, capturing and storing CO_2 in aquifers is a costly process. In addition to the cost, the storage technology has several constraints, such as pressure build-up, injection capacity, and environmental effects. Although there are some previous works separately combining CO_2 storage with brine extraction (Active CO_2 Reservoir Management, ACRM)(Aines, Wolery et al. 2011, Buscheck, Sun et al. 2011) or with geothermal power plants (CO_2-based Engineered Geothermal Systems, CO_2-EGS)(Pruess 2008, Atrens, Gurgenci et al. 2009, Atrens, Gurgenci et al. 2010, Fard, Hooman et al. 2010, Spycher and Pruess 2010), they are not systematic. In this study, we examine a new concept that combines the three components of CO_2 storage, brine extraction, and geothermal energy utilisation. The advantage of this concept is the potential to store CO_2 in an underground aquifer system with high porosity and permeability, while simultaneously providing pressure support for brine production activities. Produced brines may be used for both geothermal energy content and ions present at economic concentrations. This study is to provide the foundations for analysis of this concept. It uses as the basis the geological model of a geopressured-geothermal reservoirs developed using available data from the aquifers of Jianghan Basin (Fig.3), but it could be conceptually be applied to other thermal brine reservoir systems.

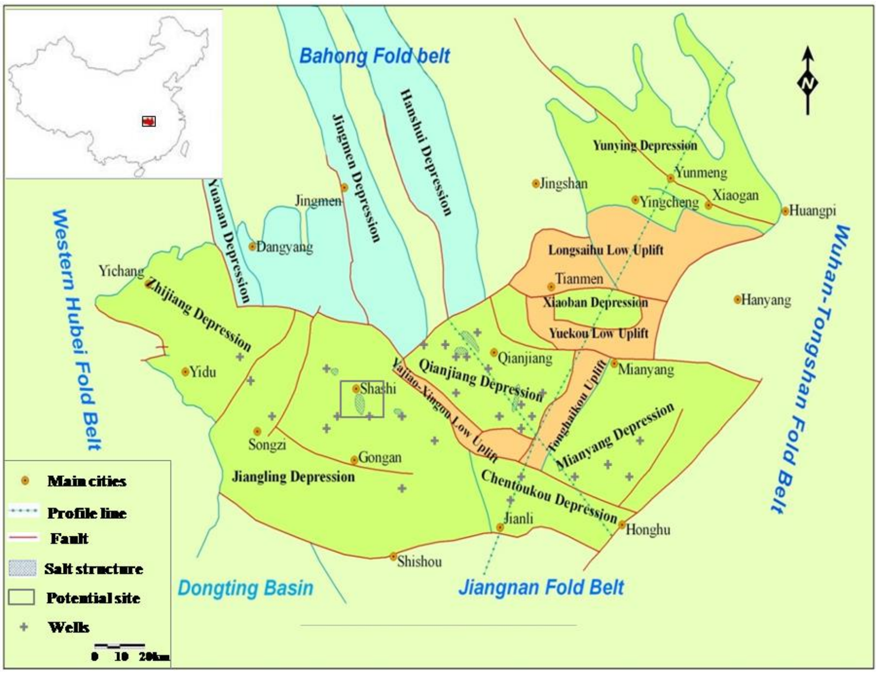

Fig.3. Location of the research area in Jianghan Basin

Formations of abnormally high pressure (nearly 80 MPa) and temperature (100 ℃) lie in the Jianghan basin of China at depth from 2500 to 3500 metres. The research zone Qianjiang Formation contains four sets of the regional seals, namely 1~6 rhythms in the Upper Qian Four, 4~8 rhythms in the Lower Qian Three, 11~15 rhythms in the Qian Two and argillaceous gypsum bed on the top of Qian One. The rhythm caprock is composed of the grey mudstone, salt rock and argillaceous gypsum. Table 2 gives a simple generalized model of the reservoir and seal pairs of Qianjiang Formation in Jiangling Depression of the Jianghan Basin.

Table2. Reservoir and seal pairs of Qianjiang Formation in Jiangling Depression, Jianghan Basin

Formation		Thickness (m)	Sandstone&Interlayer	Reservoir	Caprock
Qian 1	Mud-gypsum rock	110~450	Regional Interlayer		
	Zhouji Sandstone		Sandstone Segment 1		
	Soft-mud rock				
Qian 2	Upper Qian 2	110~700			
	11~15 rhythm		Regional Interlayer		
	Lower Qian 2		Sandstone Segment 2		
Upper Qian 3	Qian 3-1	150~640			
	Three-high resistant Fm				
	Qian 3-2				
Lower Qian 3	Qian 3-3				
	4~8 rhythm		Regional Interlayer		
	Qian 3-4		Sandstone Segment 3		
Upper Qian 4	Qian 4-1	100~700			
	2rhythm				
	Qian 4-0				
	1~6 rhythm		Regional Interlayer		
	7~6 rhythm		Sandstone Segment 4		
	Qian 4-2				
	4 rhythm				
	Qian 4-3				
Lower Qian 4	Lower Qian 4	173~2218			

The salinity of brine in the basin is on the order of 150-340 gram per litre. The brine in these formations mainly contains Na^+, K^+, Ca^{2+}, Mg^{2+}, Li^+, Cl^-, SO_4^{2-}, Br^-, I^-, and B^-. For example, The K^+ content of this brine is up to 1.6%, which is more than 1.0% of industrial mining grade can be used to produce KCl. Moreover, lithium and bromine concentration also achieve industrial grade that can be produced. The production of brine will reduce the pressure of the formations from which it is extracted. Depending on the source of the over-pressurization of the reservoir system, this reduce in pressure may occur rapidly or slowly. If it occurs rapidly, potential brine production flow rates may fall rapidly below desirable levels. This would, however, provide an opportunity for simultaneous injection of CO_2 into the same formations. CO_2 injection accompanying brine extraction would benefit from improved injection efficiency (due to a reduction in formation overpressure) and increased storage capacity for a given volume of saline formation (Buscheck, Sun et al. 2011, Klise, Roach et al. 2013). In addition, the production of this brine rich in K^+, Li^+, Br^-, I^- could help offset the cost of CO_2 sequestration. Consequently the use of CO_2 injection into this reservoir system could offer an opportunity to improve brine production rates and geothermal energy production.

Furthermore, the geothermal energy content of the hot brine is also significant. The temperature of Jianghan Basin geothermal aquifers is about 100 ℃. Therefore, geothermal energy extracted from produced brine could be used directly or potentially converted to electricity. The total energy content of the brine, for a surface temperature of 25 ℃ is approximately 314 kJ per kg of brine (estimated from pure water enthalpy). Thus, for production rates of 50-1000 kg s^{-1} (approximates of one well and a field development), this represents a substantial thermal energy flow of 15.7 MWth to 313 MWth. Assuming a second-law thermodynamic efficiency of 25%, which is conservative for geothermal power developments, the previously mentioned flows of brine could generate 0.8 MWe to 15.8 MWe of electricity.

The use of CO_2 as an operating fluid in enhanced brine extraction and geothermal energy production has been proposed as a means not only to produce "clean" energy, but also to potentially sequester CO_2 through fluid losses at depth. As this strategy offers a number of significant advantages, particularly (Atrens, Gurgenci et al. 2010):

- Inherent physical sequestration of some CO_2 as part of the operation (amount needed to fill the reservoir volume), and depending on the geology present, possibility of chemically sequestering CO_2.
- A strong buoyancy effect, whereby the static pressure change (i.e. the change in pressure due to fluid density) in the injection well is much larger than in the production well (due to higher temperatures and lower densities). This leads to high self-driven flow rates, making large pumping equipment unnecessary (although as previously noted, recompression may be economical). A system without pumping equipment is illustrated in Fig.4.
- Manage pressure build-up, the strategy of producing brine can immediately reduce or even completely avoid the pressure build-up associated with CO_2 injection.

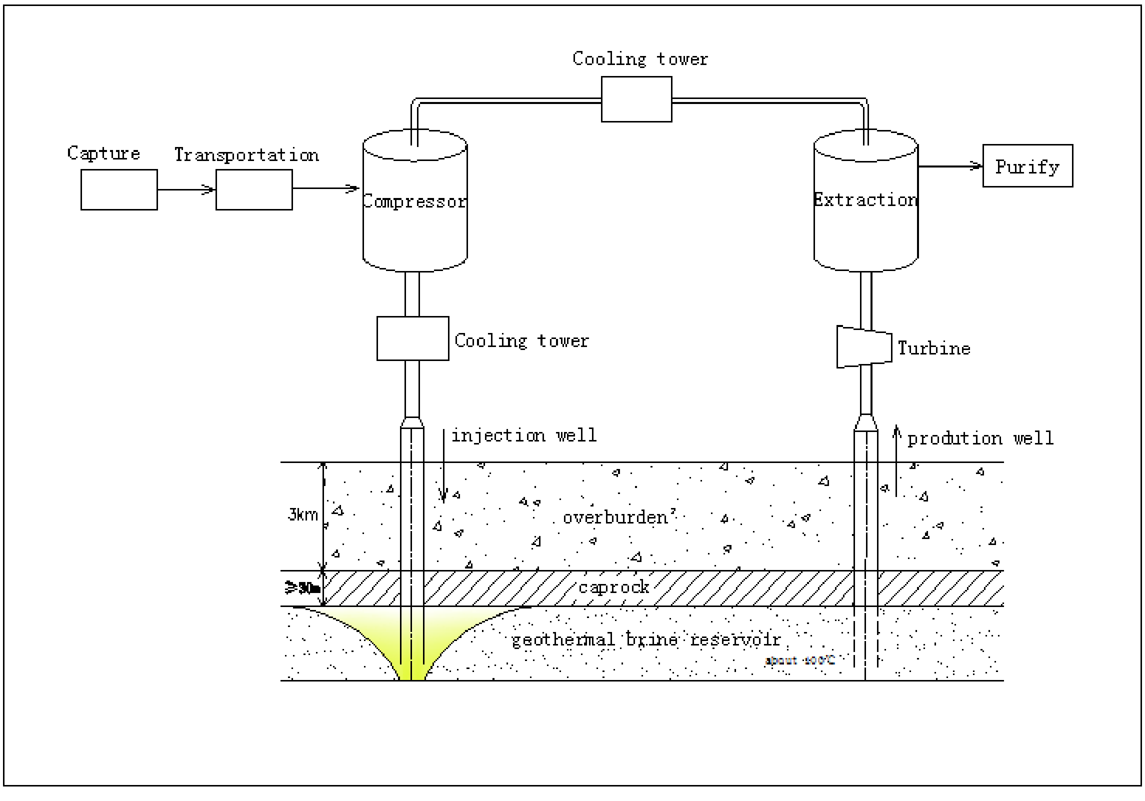

Fig.4. A system designed to extract brine and geothermal energy from geothermal reservoirs without pumping equipment

The purpose of this work is to develop an initial mass balance of a segment of the reservoir system in the Jianghan Basin, China. This mass balance can provide order of magnitude estimates of the total quantity of CO_2 that can be stored in the Basin, total quantities of brine extracted as well as thermal energy content contained in the extracted brine. Additionally, by considering different flow-rates for produced brine, injected CO_2, and subsurface flows at the boundary of the reservoir segment, the balance can assess the relevant time-scales for substantial alterations in reservoir fluid composition. This mass balance and associated approach can then be used as a foundation for other work to assess the potential for this concept in the Jianghan Basin or elsewhere. Reservoir models predicting injection or production flows and their relation to reservoir pressure can be linked to a mass balance model of this type.

3.2 Methodology

To address this issue, a conceptual model is needed to describe the fluid complexities of this process and examine the pressure change in such a system. The model used is simple to allow for an analytical solution, and to allow for straightforward examination of the relevant parameters.

Several models have been proposed for reservoirs, which may be very accurate with specific reservoir data but limited by their levels of sophistication. Our original model is developed by Atrens et al. A conceptual diagram of this model is shown in Fig.5. This model consists of the injection well, production well and a constant volume of free space (V_{RES}) within the 'operational' volume of the reservoir. We use the term 'operational' to keep this region distinct from other regions of the reservoir to which it may be connected. Into this reservoir, carbon dioxide is injected at a constant rate, $\dot{m}_{CO2inj}$. In reality, it would probably be preferable, due to CO_2 source reasons, to inject at a constant pressure, indicated in Fig 5 as P_{inj}, in particular because exceeding the minimum stress for tensile failure in the reservoir could result in hydraulic fracturing, which could result in creating fluid flow pathways out of the reservoir through seal layers. A constant flow rate of brine, $\dot{m}_{brineout}$ flows out of reservoir into the production well. In the reservoir system, subsurface flows are possible, consisting of CO_2 loss to surrounding reservoir segments, $\dot{m}_{CO2loss}$, and net brine influx $\dot{m}_{brinenet}$, which could consist of outflow, in which case it would take a negative value.

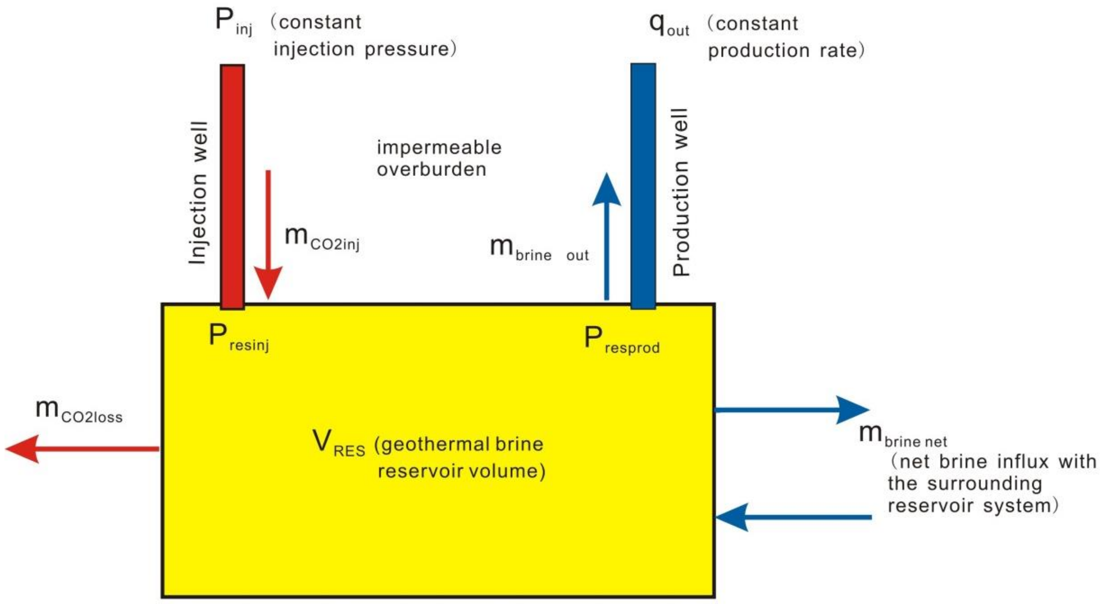

Fig.5. Conceptual diagram of model

This model is fundamentally a mass balance of the fluid contained in an individual reservoir segment. The boundaries of the reservoir segment are arbitrarily defined, but have direct consequential effects on what possible or reasonable values may be taken by subsurface flows. The model specifically does not take into account local time-dependent pressure behaviour governed by fluid flow characteristics. For small, highly permeable, and well-confined reservoir volumes, this approach is more characteristic of behaviour, but for large, less-permeable aquifers with long-ranging connectivity, substantial time-dependent pressure changes make the outputs of calculations of this model less meaningful. For systems of that type, it is critical to couple this with comprehensive radial flow modelling to elucidate local transient pressure-flow relations.

3.2.1 Model calculations

MATLAB is used to calculate the outputs of the simulated mass balance for defined input parameters. Calculations are analogous to material balance equations used in petroleum industries as a fundamental reservoir engineering tool (Havlena and Odeh 1963); those methods are used to empirically test for a number of potential drive mechanisms given known production data by rearranging the material balance equation to result in an equation of a straight line. Here we substitute possible flow rates into a similarly formulated balance to evaluate how alterations to overall system flow affect long-term outcomes for the system. If combined with data from flow performance tests or brine production, this approach could be re-used to evaluate likely usefulness of CO_2 injection to maintain reservoir pressures. The Helmholtz free energy-based equation-of-state and modified Peng-Robinson equation-of-state were used to model the PVT properties of CO_2 and water. However, brine density was assumed to be a constant (100 ℃, 30 MPa) in this calculation. While mixed phase regions are important for reservoir flow behaviour, they are less critical to the material balance of substance present in the reservoir system. These correlations cover the thermodynamic and transport properties of these fluids over the range of temperatures and pressures in this study.

3.2.2 Injection

The relationship between the injection pressure and the mass flow, which is derived from the fluid mechanics of pipe flow in the injection well, and Darcy flow in the reservoir (Span and Wagner 1996, Paulus and Penoncello 2006, Atrens, Gurgenci et al. 2010). The injection temperature at the wellhead is generally assumed to be that of the ambient, potentially plus some nominal temperature difference due to heat exchanger inefficiencies. The wellhead injection pressure is constant. The pressure change in a flowing well utilizes the wellbore model modified from (Brill and Mukherjee 1999, Pruess 2006, Atrens, Gurgenci et al. 2010), which takes into account the hydrostatic pressure and the frictional pressure drop terms along the wellbore. Starting at the injection wellhead, an injection pressure P_{inj}, and a mass flow rate, m are set. The injection pressure at bottom-hole in the reservoir can be represented by:

$$P_{resinj} = P_{inj} + \rho g \Delta z + \Delta P_f \tag{1}$$

The pressure loss due to friction can be calculated with the Darcy–Weisbach equation:

$$\Delta P_f = f \frac{\Delta z}{D} \rho \frac{V^2}{2} = f \frac{8m^2 \Delta z}{\pi^2 \rho D^5} \tag{2}$$

Where
ΔP_f is the frictional pressure drop along the wellbore (*Pa*); ρ is the density of the fluid, (kg/m^3); g = 9.81m^2/s is the gravitational acceleration; Δz is the change of well depth (m); D is the internal diameter of the well (m); f is the Darcy friction factor, which is assumed to be constant; and V is the fluid velocity (m/s).

While determination of the injection pressure behaviour is not necessary with assumed mass flow rates, the above equations can determine the injection pressure necessary to achieve a given wellbore flow or bottom-hole pressure, and vice-versa. This can consequently be used in conjunction with a reservoir flow model to determine either the injection pressures necessary to meet CO_2 flow requirements, or the number of wells necessary if injection pressure is limited (either by surface facility capabilities or by the fracturing stress of the reservoir).

3.2.3 Reservoir

In the application of the mass balance equation we are assuming that the pressure is uniformly distributed across the reservoir. If there is uniform pressure decline in all the wells in the reservoir then this pressure decline gives confidence for application of the mass balance tool. Dake (Dake 2001) pointed out that if this equilibrium is not achieved, the mass balance approach can still be used. He suggested that an average pressure can be determined to represent a reservoir where there are large differential pressures across the reservoir.

As we observed in this study, with CO_2 drive (CO_2 injection) CO_2 will enter pore volume originally occupied by brine, and the produced fluids are now brine with its contained solution CO_2 and CO_2 which has come out of solution from the brine. We assume firstly that there is no substantial change in the free space available within the reservoir segment, i.e. that the net effect of any dissolution or precipitation of minerals, or pore expansion or compression are minimal. We also assume that there are no components present aside from brine and CO_2, and that the net balance of injection, production, and subsurface flows are sufficient to maintain a specified average reservoir pressure. Consequently, a simplified material balance for this system can be expressed as:

Present brine volume = original brine volume – reservoir volume of CO_2 injection – CO_2 loss – brine produced + net brine influx with the surrounding reservoir system

$$V_{RES} = V_{RES} + V_{CO2inj} - V_{CO2loss} - V_{H2Opro} + V_{H2Onet} \tag{3}$$

This can be converted to:

$$\frac{\dot{m}_{CO2inj}}{\rho_{CO2}} - \frac{\dot{m}_{CO2loss}}{\rho_{CO2}} - \frac{\dot{m}_{H2Opro}}{\rho_{H2O}} + \frac{\dot{m}_{H2Onet}}{\rho_{H2O}} = 0 \tag{4}$$

The temperature in the reservoir is assumed to be constant. The model formulation is summarized below to analyse the described system.

The 'operational' volume of the reservoir is expressed by:

$$V_{RES} = \phi \cdot H \cdot L \cdot W \tag{5}$$

Where

ϕ is the porosity of the reservoir; H is the height of reservoir (m); L and W are the surface dimensions of the reservoir segment considered.

$$\frac{dM_{CO2}}{dt} = \dot{m}_{CO2inj} - \dot{m}_{CO2loss} \tag{6}$$

$$M_{CO2} = \dot{m}_{CO2inj} \times t - \dot{m}_{CO2loss} \times t \tag{7}$$

For completeness, the mass of brine in the reservoir can be defined by the equation:

$$\frac{dM_{H2Ores}}{dt} = \dot{m}_{H2Opro} - \dot{m}_{H2Onet} \tag{8}$$

$$M_{H2O} = M_{H2Oinit} - \dot{m}_{H2Opro} \times t + \dot{m}_{H2Onet} \times t \tag{9}$$

$$M_{H2Oinit} = \rho_{H2O} \times V_{RES} \tag{10}$$

$$X_{CO2} = \frac{M_{CO2}}{M_{CO2} + M_{H2O}} \tag{11}$$

The mass fraction X_{CO2} can be considered therefore as a dimensionless expression for time for the reservoir system. It can therefore be transformed to determine actual time, dependent on the individual flow rates:

$$t = \frac{M_{H2Oinit} \times X_{CO2}}{\dot{m}_{CO2inj} - \dot{m}_{CO2loss} - X_{CO2}(\dot{m}_{CO2inj} - \dot{m}_{CO2loss}) + X_{CO2}(\dot{m}_{H2Opro} - \dot{m}_{H2Onet})} \tag{12}$$

$$V_{RES} = V_{CO2} + V_{H2O} = \frac{M_{TOT} \times X_{CO2}}{\rho_{CO2}} + \frac{M_{TOT} \times (1 - X_{CO2})}{\rho_{H2O}} \tag{13}$$

$$M_{TOT} = \frac{\rho_{CO2} \times \rho_{H2O} \times V_{RES}}{X_{CO2} \times \rho_{H2O} + (1 - X_{CO2}) \times \rho_{CO2}} \tag{14}$$

Where
M_{CO2} is the total mass of CO_2 in the reservoir operational volume (kg), M_{H2O} is the total mass of brine in the reservoir operational volume (kg), M_{TOT} is the total mass of fluid in the reservoir operational volume (kg), X_{CO2} is mass fraction of CO_2 in the reservoir, $\dot{m}$ is the mass-flow rate of the fluid (kg/s), ρ is the fluid density (kg/m^3).

The thermal heat of produced brine can be calculated by:

$$Q = c_p \times M_{H2Opro} \times \Delta T \tag{15}$$

Where
c_p is the specific heat capacity of brine (J/(kg K)), ΔT is the temperature change between geothermal aquifers and surface temperature (K).

For an incompressible reservoir without dissolution or precipitation effects, the average pressure of the reservoir is a function directly of the volume of free space in the reservoir, the quantity of different fluid types contained in the reservoir, and the fundamental P-V-T relations of those fluids. If the brine density does not depend on pressure, reservoir pressure depends only on the relationship between pressure and density of CO_2:

$$P_{RES}(t) = f(V_{RES}, T_{RES}, \rho_{CO2res}, X_{CO2}) \tag{16}$$

If brine density is varied on the basis of known data, a generalised brine equation of state, or based on the equation of state for pure water and adjusted for dissolved solids, then it must also be included in the relation above. If the mixed phase region is also considered, then the density of CO_2 containing water, and water containing CO_2 at the relevant concentrations, and their proportions must also be included.

For the purposes of this model, we have taken a range of final ‘desired’ reservoir pressures, calculate the densities of CO_2 and brine, and from this determine the quantities of fluid that can be contained within the fixed reservoir volume for a defined overall composition. This is then what provides the basis for the time-X_{CO2} relations described above. The exception is a case without CO_2 injection; it can easily be shown that the change in brine density between initial and final pressure, multiplied by total reservoir volume and divided by brine production flow is explicitly the production time for such a case.

3.2.4 Production

The brine production at the wellhead is assumed to be at a constant mass flow rate. Fluid transfer from the operational zone of the reservoir to the wellhead can be modelled by pipe flow in the production well, in which the production pressure, P_{prod} is calculated from:

$$P_{prod} = P_{resprod} - \rho g \Delta z - \Delta P_f \tag{17}$$

Where
$P_{resprod}$ is the production pressure at downhole in the reservoir (*Pa*). The frictional pressure drop in the production well is calculated in the same manner as for the injection well, using Eqs. (2).

Combining Eqs. (2) and (17) allows calculation of the production wellhead pressure for any mass-flow rate. While not strictly necessary to solve the reservoir model which defines a constant brine production flow rate, this calculation should be used to ensure that production pressures are not lower than the flash pressure of the brine. If they are, very substantial precipitation of dissolved material can occur in the production well. While there are techniques to circumvent this issue, it will generally be more favourable to produce at flow rates sufficiently low to ensure brine remains below the saturation pressure.

Parameter values for the Jianghan Basin for these sets of equations for the simulation are listed in Table 3.

Table3. Reference parameters

Properties	**Values**
Depth (m)	2500~3500
Single thickness (m)	100
Total thickness (m)	1800
Reservoir volume (m^3)	$5\sim29\times10^9$
Reservoir temperature (^oC)	100
Geothermal gradient （$^oC/100m$）	3.0
Reservoir pressure (MPa)	80
Reservoir permeability κ (m^2)	10^{-13}
Pore compressibility (Pa^{-1})	4.5×10^{-10}
Porosity	0.18
Rock grain density (kg/m^3)	2600
Formation heat conductivity (W/m/K)	2.51
Salinity (g/L)	100~340
Injection temperature (℃)	25

3.3 Assumptions

The analysis described in this paper is based on a number of assumptions:

- The system is at mechanical equilibrium – i.e. no internal pressure gradients;
- There is no existing gas cap providing pressure support;
- The brine has a density equivalent to pure water;
- The region of mixing of CO_2 & brine is small, achieved preferably by injecting CO_2 up-dip in shallower regions of relevant aquifer layers;
- The reservoir has been assumed to be homogeneous, which is unlikely to be the case in reality; and
- The effects of localised changes in permeability on CO_2 and brine flows, and their interaction in terms of relative permeability effects, have not been examined in this work.

Additionally, as noted previously, this analysis, taken without reservoir flow models, is fundamentally appropriate for reservoir volumes that are small, highly permeable, and well-confined (which allows the model to meet the mechanical equilibrium assumption above).

3.4 Results

It is trivial to determine the amount of total mass, and masses of brine and CO_2 contained in the reservoir for different equilibrium reservoir pressures, as described in the method. First, we examine the basic behaviour of the system described, which is that of specified reservoir volume V_{RES}, initial brine density ρ_{H2O}, input mass flux $\dot{m}_{CO2in}$, and output brine flux $\dot{m}_{H2Opro}$ towards different equilibrium pressures. The density of CO_2 as a function of pressure at 100 ℃ was calculated from Helmholtz free energy equations of state (coded in Matlab as co2eqofstate.m). The effect of system parameters on the modelled system are examined to determine how system behaviour changes in response. In this study, we have plotted calculation results for these quantities as functions of mass fraction of CO_2, but as described above it can be transformed to a measure of time.

3.4.1 Reservoir pressure

To calculate the relationship between amount of substance and reservoir pressure, we normalised the results by reservoir volume to provide a generalised result applicable to the bounded reservoir systems of interest. We assume that the system contains no influx or outflow of fluid at the edges of the reservoir.

Shown in Fig.6 is the total mass of fluid contained in the specified reservoir volume as a function of CO_2 mass fraction.

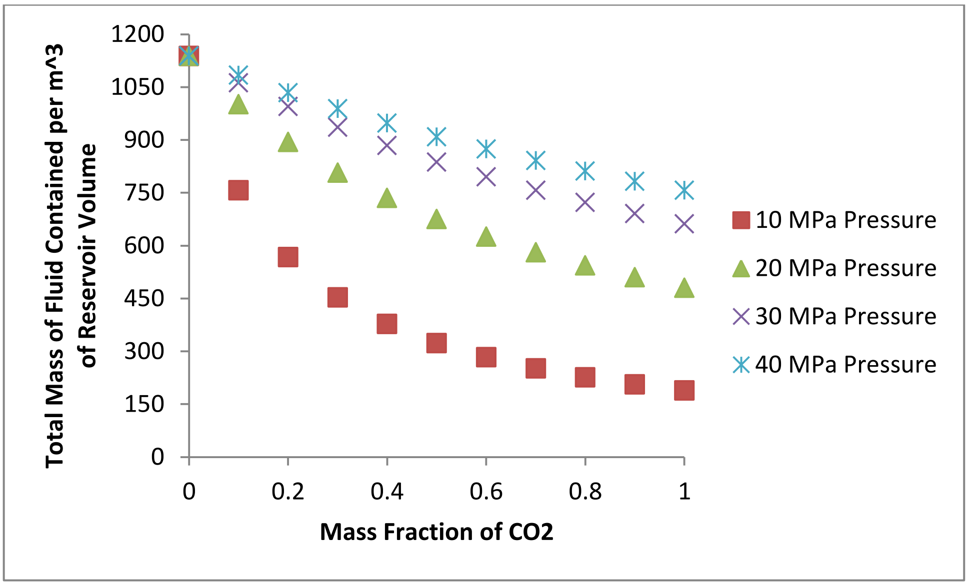

Fig.6. Total mass of fluid contained per m^3 of reservoir volume versus CO_2 mass fraction

From Fig.6, we note that there is a great change of total mass of fluid contained in reservoir as the different equilibrium reservoir pressures. At low pressure (10MPa), there is asymptotic behaviour in response to CO_2 mass fraction. At higher pressure (40MPa), it shows that total mass of fluid contained in reservoir is nearly direct proportional to CO_2 mass fraction. Final reservoir pressure alters the total quantity of fluid that can be stored in the reservoir system. If the final system is filled with CO_2, it does not alter the quantity of brine that can be extracted. It does however alter the quantity of CO_2 that can be stored.

The effect of CO_2 mass fraction on the amount of CO_2 injectable and brine extractable for different equilibrium reservoir pressures are shown below. It is evident that the equilibrium reservoir pressure has a greater effect on the quantity of CO_2 stored in reservoir compared to brine extracted from reservoir. When there is no underground flux at the edges of the reservoir, the maximum amount of brine that can be extracted is 5.15 kg per m^3 of reservoir volume for a reduction in average pressure from 30 MPa down to 20 MPa.

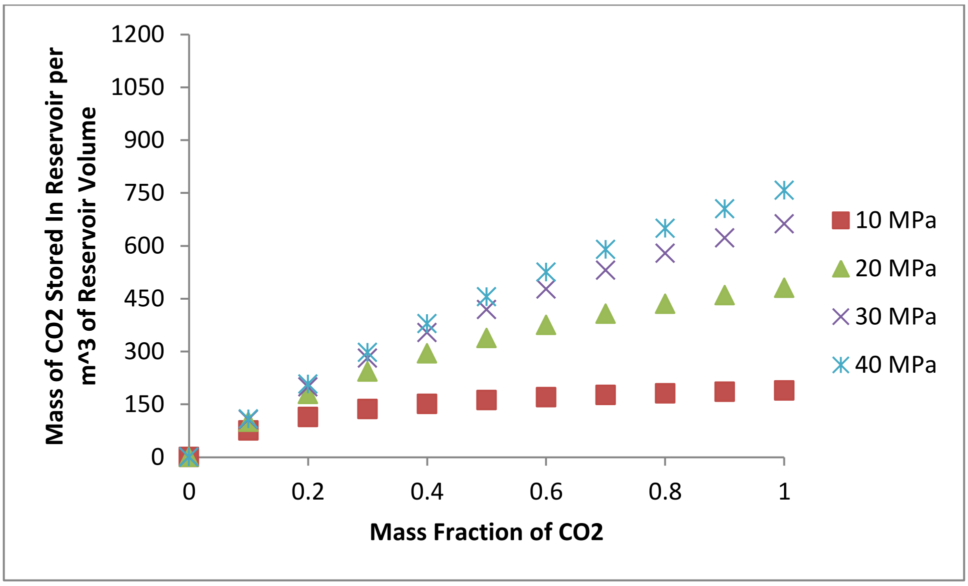

Fig.7. Mass of CO_2 stored per m^3 of reservoir volume versus mass fraction of CO_2

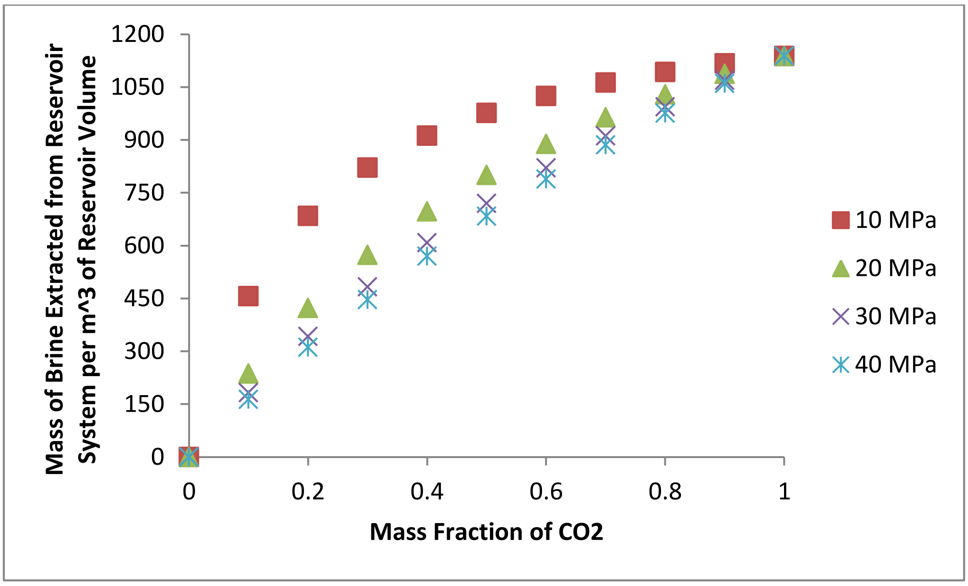

Fig.8. Mass of brine extracted per m^3 of reservoir volume versus mass fraction of CO_2

For the same reservoir volume, an injection of just 9.95 million tons of CO_2 would enable extraction of 17.12 million tons of brine (interpolated from results, for a mass fraction X_{CO2} of 0.01 and reservoir pressure 30 MPa) without any reduction in reservoir pressure.

3.4.2 Change in flow at the reservoir boundaries

Also, the mass fraction X_{CO2} can be considered as a dimensionless expression for time for a reservoir system. In order to convert X_{CO2} into an actual time value for specified flow rates and total reservoir volume, we consider, as per the assumptions that the effect of influx simply displaces brine at the reservoir boundaries at the equilibrium reservoir pressure of 30 MPa. Now we consider the change of the relationship between time and X_{CO2} for different CO_2 and brine mass flows. In the following four different cases are considered.

Case 1: No influx or outflow of fluid at the reservoir boundaries

Assuming no influx or outflow of fluid at the reservoir boundaries, we can, for constant reservoir conditions, easily calculate the relationship between time and CO_2 mass fraction.

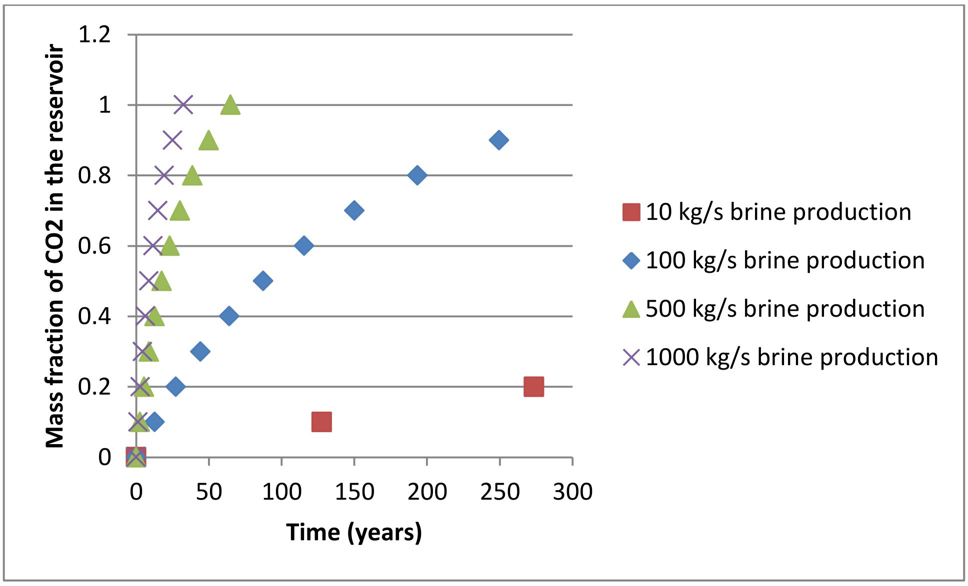

Fig.9. Mass fraction of CO_2 versus time for different brine production rates

It is evident from Fig.9 that larger brine production rates offer an opportunity to reduce the time scale with the mass fraction of CO_2. The mass fraction of CO_2 increases strongly over time at the brine production rate of 1000 kg/s, and the time scale is no more than 33 years until the entire reservoir is filled with CO_2. However, it needs a long time for CO_2 to replace the entire brine from the reservoir when the brine production rate is very low (i.e. it will take more than 3000 years at the brine production rate of 10 kg/s).

Case 2: No CO_2 loss, with net brine influx at the reservoir boundaries

The effect of net brine influx on the CO_2 mass fraction for the system is shown in Fig.10.

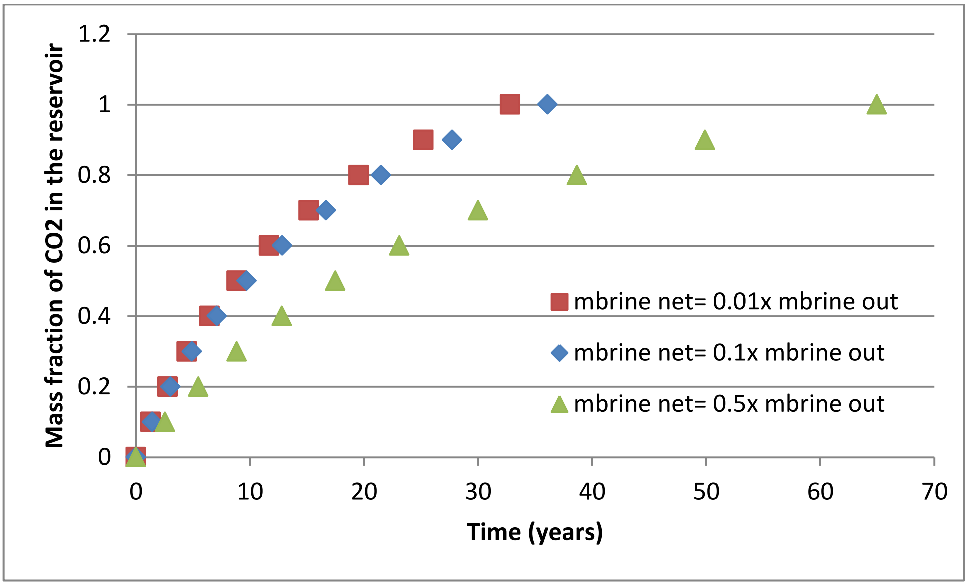

Fig.10. Mass fraction of CO_2 versus time for different ratios of net brine influx/brine production

From Fig.10, we note that as water influx at the boundaries of the reservoir increases, the length of time for sustained production is greatly increased. However, the amount of CO_2 injection decreases. What this means is that instead of injecting CO_2, brine from elsewhere is providing the drive for production flows.

Case 3: No net brine influx or outflow, with CO_2 loss at the reservoir boundaries

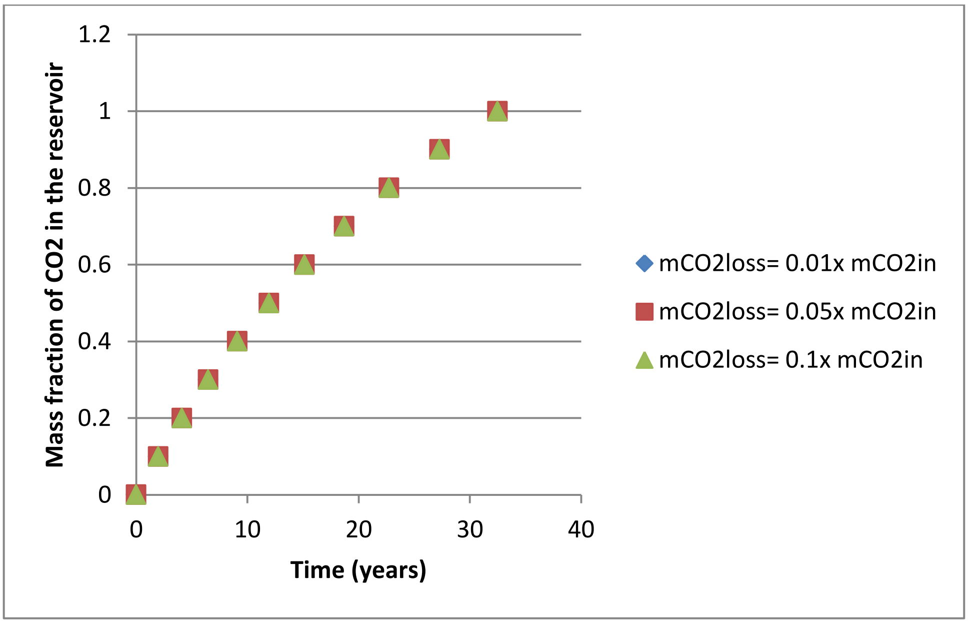

Fig.11. Mass fraction of CO_2 versus time for different ratios of CO_2 loss/CO_2 injection

As seen in Fig.11, CO_2 loss has negligible influence on CO_2 mass fraction in the reservoir. However, the method in which results are presented hides the significance of CO_2 loss. It should be noted that this behaviour is not a simulacrum of reality. As CO_2 loss increases, increased CO_2 injection would be expected to provide a constant reservoir pressure. This behaviour results as shown in Fig.12.

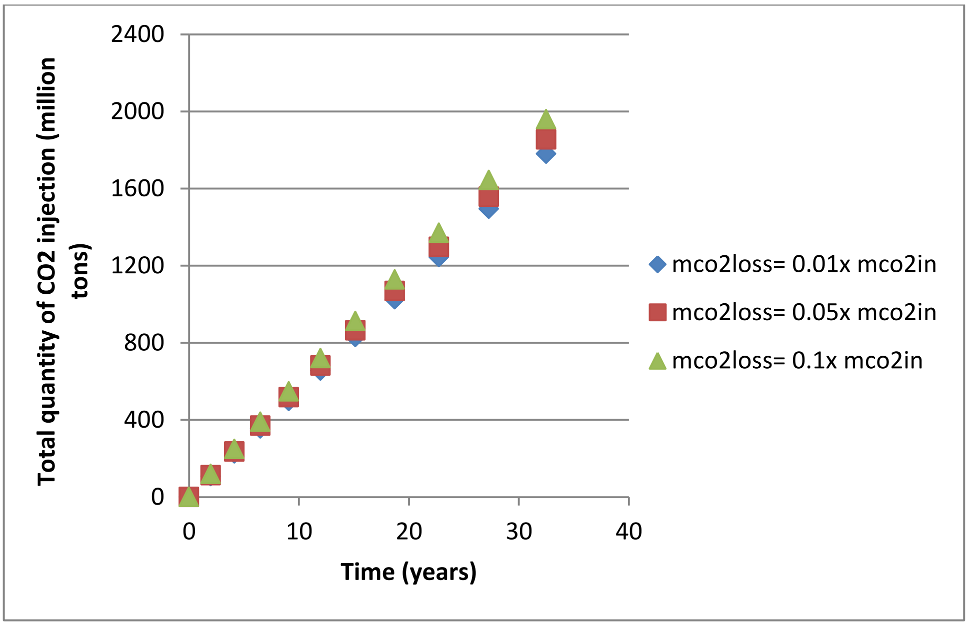

Fig.12. Total quantity of CO_2 injection versus time for different ratios of CO_2 loss/CO_2 injection

Fig.12 shows that total quantity of CO_2 injection is directly proportional to time. For different ratios of CO_2 loss/CO_2 injection, the maximum time scales which are the same are nearly 33 years. Note that the increased CO_2 loss leads to a substantive increase in CO_2 injection, and the total quantity of CO_2 injection increases from 1780.06 million tons to 1958.07 million tons as the ratio of CO_2 loss/CO_2 injection increases from 0.01 to 0.1.

Case 4: With CO_2 loss and net brine influx or outflow at the reservoir boundaries

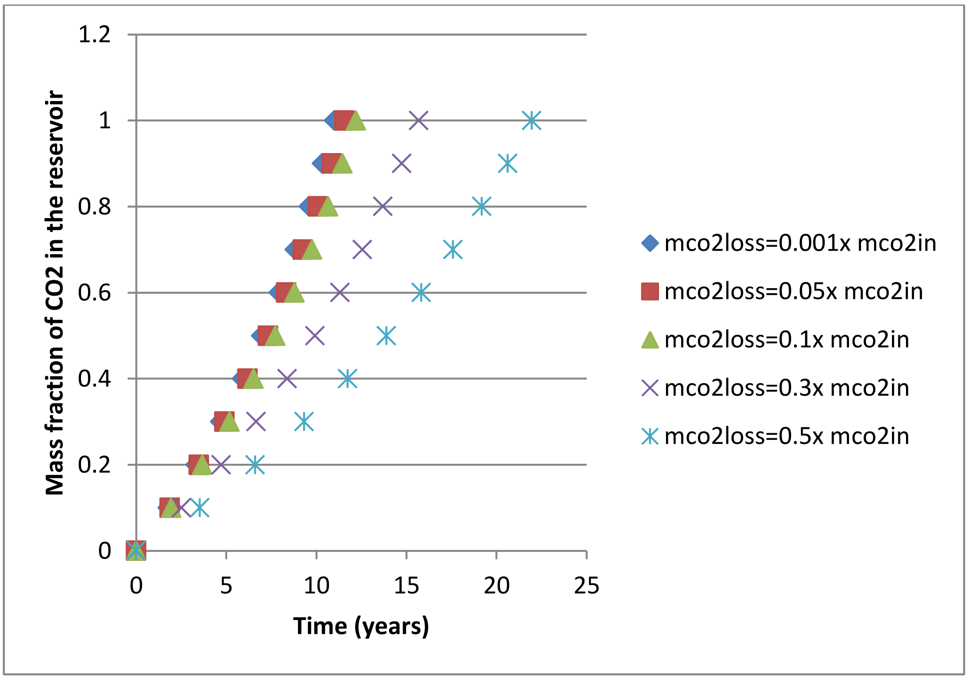

Fig.13. Mass fraction of CO_2 versus time for different ratios of CO_2 loss/CO_2 injection

It is can be seen from Fig.13 that CO_2 loss has great influence on time scale for entire reservoir is filled with CO_2. The time scale becomes longer as CO_2 loss increases. However, this behaviour is different from case 3 (see Fig.11) which time scale is constant for different ratios of CO_2 loss/CO_2 injection. This happens to some extent influenced by net brine outflow.

Using modified equation 4, we calculate the total quantity of net brine outflow underground over the lifetime of the reservoir. The results of this calculation are shown in Fig.14.

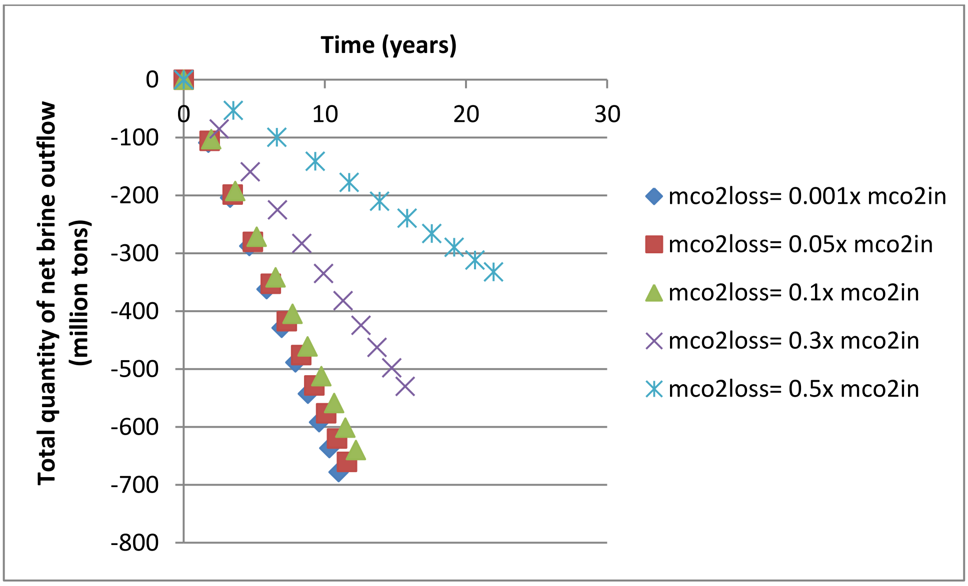

Fig.14. Total quantity of net brine outflow versus time for different ratios of CO_2 loss/CO_2 injection

Note that the value of total quantity of net brine is negative, so we can determine that there is outward flow of brine from the reservoir. From Fig.14, we can see that as CO_2 loss increases, total quantity of net brine outflow decreases, while time scale increases. This happens because when CO_2 loss increases, the reservoir pressure will decrease for the mass of CO_2 injection is constant.

3.4.3 Geothermal energy content

The geothermal energy content of the hot brine can be calculated by equation 15. The specific heat capacity of brine is 4.18 kJ/(kg·K), the temperature of Jianghan Basin geothermal aquifers is about 100 ℃. Therefore, the total thermal heat of brine, for a surface temperature of 25 ℃ is approximately 313.5 kJ per kg of brine (estimated from pure water enthalpy).

For production rates of 50~1000 kg s^{-1} (approximates of one well and a field development), this represents a substantial thermal energy flow of 15.7 MWth to 313 MWth. Due to the low temperature of the brine, it is not highly-suited to electricity generation, but there is precedent, such as the Birdville Geothermal Plant in central Australia, and there may be direct local needs for generated electricity in brine processing industries. The Carnot efficiency for a source temperature of 100 ℃ and a sink temperature of 25 ℃ is ~20.1%. Assuming a second-law thermodynamic efficiency of 25%, which is conservative for geothermal power developments, the potential electrical output is 5% of thermal heat flow, the previously mentioned flows of brine could generate 0.8 MWe to 15.8 MWe of electricity.

Furthermore, injection of CO_2 could assist in maintaining constant reservoir pressures to prevent flow decrease with time, and as the reservoir is filled with CO_2, it could eventually be used as the heat extraction fluid itself.

3.5 Discussion

We specified the brine production rate as 10, 100, 500 and 1000kg/s to test the time scales over which the reservoir system of the specified volume would maintain sustainable production. The rate of 100kg/s is expected for brine production from a single well in the reservoir system. However, for a field-scale development, the brine production rate 1000 kg/s can be a reference. The length of time for brine (K^+, Li^+, Br^-, I^-) extraction could reliably be produced is about 30-60 years.

The actual brine area is about 960 km^2, and the average thickness of reservoir is nearly 500 m. The surface area might be accessed by a single well is 10000 m^2, the area that might be accessed by a field consisting of multiple wells is about 16 km^2, although this is uncertain. For a porosity of 0.18, the nominal V_{RES} specified in these calculations of 9×10^8 m^3 is equivalent to 10,000,000 m^2 or 10 km^2. It is of the same order of magnitude as a field development, and supports assessment of produced brine flow-rates on the order of 100 to 1000 kg/s.

Effectively, water influx directly supports sustained brine production. Brine production without CO_2 injection can proceed indefinitely at whatever subsurface water flow-rate can be maintained by water drive. Consequently if the reservoir system is well-connected over very large distances to over-pressured water sources of substantial volume, CO_2 injection will be of minimal importance to maintain reservoir pressures. It may still be favourable to inject CO_2 if an overall increase in average reservoir pressures beyond that provided by the water drive is desirable. Furthermore, water influx is unlikely to be a constant rate, but will be dependent on a relationship between the water source and average reservoir pressure.

Based on the currently available data for the Jianghan Basin, it is difficult to determine the likely water influx into an arbitrary segment of the reservoir system, or in fact of the intra-connectivity of the reservoir generally, and how it is linked to other nearby aquifers. The over-pressures present in the reservoir system could be due to compression, connectivity to deep water sources, or long-distance connectivity to a gas cap. Production history from the early stages of the production wells and pressure measurements in the reservoir could provide hints as to which mechanisms are present, and will have associated implications for the usefulness of CO_2 injection. However, in Case 4, there is outward flow of water from the reservoir, it imply that higher injection flow rates of CO_2 could be achievable without rapidly increasing reservoir pressure.

In terms of the relationship between time and CO_2 presence in the reservoir, the results as presented do not look impressive. However, the method in which results are presented hides the significance. Because calculations progressed from an assumption of maintained reservoir pressure, as CO_2 losses increase, a substantial increase in CO_2 injection is required to provide a constant reservoir pressure and therefore sustained brine production rates.

Whether this type of loss of CO_2 is favourable or not should contrast with Carbon Capture and Storage when not combined with brine extraction and geothermal utilisation. The magnitude of CO_2 losses is of course a significant topic for future research. As noted by this analysis, the CO_2 must occupy some volume. If this involves physical flow, it will have pressure effects on the reservoir or will alter other flow parameters such as water influx. If it is due to chemical reactivity with reservoir rocks, it may both alter porosity (altering free pore space), permeability and consequent flow behaviours, and will of course be dependent on the reservoir mineralogy. The CO_2 loss will be fundamentally linked with water influx/ or outflow, as both depend on long-range connectivity and a relation between the average reservoir pressure and the pressure of pore and fracture spaces connected to the reservoir system. There is an additional complexity that CO_2 losses would be expected to only occur upwards or laterally from the reservoir system due to its lower density than brine or water. Regardless, this provides a useful starting point compared to an assumption of a continuous constant loss rate or percentage of injected CO_2.

There is a large change in the mass of brine produced from the reservoir depending on final equilibrium reservoir pressures. At low pressure (10 MPa), there is asymptotic behaviour in response to mass fraction of CO_2. At higher pressure (40 MPa), that mass of brine produced from reservoir is nearly direct proportional to mass fraction of CO_2. When there is no underground flux at the edges of the reservoir, and without CO_2 injection, the maximum amount of brine that can be extracted is 5.15 kg per m^3 of reservoir volume for a reduction in average pressure from 30 MPa down to 20 MPa.

3.6 Conclusions

Overall, it can be concluded from this analysis that:

- If the system is well-connected to a strong water drive (i.e. comparable to desired production flow-rates of brine), then injection of CO_2 may be of minimal utility;
- If the system is confined, or if it is connected to a weak water drive or small gas cap, the injection of CO_2 can very effectively maintain reservoir pressures; and
- The quantity of CO_2 injected into a system without a strong water drive may be very substantial, and the efficacy of CO_2 storage will be greatly promoted by the removal of existing brines from the system, unless those brines can be very easily forced elsewhere in the subsurface.

Because the K^+ content of this brine is up to 1.6%, it is more than 1.0% of industrial mining grade, and an economic income of K^+ and the other elements could be calculated. This can be combined with determination of potential value for electricity conversion of the thermal energy contained in the brine, and together these can be incorporated with the cost of sequestration to approximate overall economic value of this concept.

4. Challenge and future work

There are still complexity and uncertainty for CO_2-EGS from theory to practical application, such as technical maturity, potential of scaling, economic feasibility, the amount of CO_2 storage, and the environmental impact. Future work should focus on:

- Understanding the behaviour of multiphase flows and the process of heat transfer, for example the manner in which CO_2 immiscibly displaces water within the reservoir system, CO_2 dissolution in water, water dissolution in supercritical CO_2, and how these behaviours alter the expected performance of a hybrid CO_2-geothermal-brine processing facility;
- Analysing the geochemical interactions of CO_2 with reservoir geology. In particular there are significant interactions between supercritical CO_2-water-rock resulting in mineral dissolution and precipitation, and changes of the reservoir characteristics, which may have significant implications in terms of sequestration of CO_2, and flow behaviour within the reservoir.
- Establishing more accurate and flexible model and system to describe the principle and technical feasibility of CO_2-EGS according to actual reservoir parameters, in particular combining this mass balance model with reservoir models tailored to the reservoir system to better estimate expected flow behaviours;
- Empirically evaluating the performance of CO_2-EGS currently. It is need to conduct industrially-relevant laboratory and field tests to obtain the relevant parameters and experience to verify and improve the theory and model. In particular, field tests will greatly assist in determining reservoir parameters and establishing the reliability of the concept.
- Economic potential of the system is still not well understood. It is critical for economic analyses of CO_2-EGS to include well (injection and production well) costs, CO_2 price, the income of geothermal power outputs and brine processing industries, and carbon tax and pricing mechanisms; and
- The engineering practice of CO_2-EGS requires multidisciplinary in-depth study, involving for example drilling technology, reservoir fracturing technology, energy conversion technology.

Acknowledgments

I am grateful to Aleks D. Atrens for guiding me to do this work, as well as to Yilian Li for an internal review of this report. This study was supported by a bilateral project China Australia

Geological Storage of CO_2 Project Phase 2 (CAGS2), jointly managed by Geoscience Australia and the Administrative Centre for China's Agenda 21, China, and sponsored by Geoscience Australia. I would like to extend my most sincere thanks to the project manager Liling Huang for her great help during this training. I want to express sincere thanks to Andrew Barrett, as well as Sizhen Peng, Li Jia for their support in this exchange program. I also thank Queensland Geothermal Energy Centre of Excellence, University of Queensland (QGECE) and China University of Geosciences (Wuhan) for providing the research environment.

Reference

Aines, R. D., T. J. Wolery, W. L. Bourcier, T. Wolfe and C. Hausmann (2011). Fresh water generation from aquifer-pressured carbon storage: feasibility of treating saline formation waters. 10th International Conference on Greenhouse Gas Control Technologies. J. Gale, C. Hendriks and W. Turkenberg. Amsterdam, Elsevier Science Bv. **4:** 2269-2276.

André, L., V. Rabemanana and F.-D. Vuataz (2006). "Influence of water–rock interactions on fracture permeability of the deep reservoir at Soultz-sous-Forêts, France." Geothermics **35**(5–6): 507-531.

Apps, J., Pruess, K. (2011). Modeling geochemical processes in enhanced geothermal systems with CO2 as heat transfer fluid. Proceedings of the Thirty-sixth Workshop on Geothermal Reservoir Engineering, Stanford University, Stanford, CA.

Atrens, A. D., H. Gurgenci and V. Rudolph (2009). "CO2 Thermosiphon for Competitive Geothermal Power Generation." Energy & Fuels **23**(1): 553-557.

Atrens, A. D., H. Gurgenci and V. Rudolph (2010). "Electricity generation using a carbon-dioxide thermosiphon." Geothermics **39**(2): 161-169.

Atrens, A. D., H. Gurgenci and V. Rudolph (2011). "Economic Optimization of a CO2-Based EGS Power Plant." Energy & Fuels **25**(8): 3765-3775.

Borgia, A., K. Pruess, T. J. Kneafsey, C. M. Oldenburg and L. H. Pan (2012). "Numerical simulation of salt precipitation in the fractures of a CO2-enhanced geothermal system." Geothermics **44**: 13-22.

Brill, J. P. and H. K. Mukherjee (1999). Multiphase Flow in Wells. Richardson, TX, USA, Henry L. Doherty Memorial Fund of AIME, Society of Petroleum Engineers Incorporated.

Brown, D. (2000). "A hot dry rock geothermal energy concept utilizing supercritical CO 2 instead of water." Proceedings of the Twenty-Fifth Workshop on Geothermal Reservoir Engineering: 233-238.

Buscheck, T. A., Y. W. Sun, Y. Hao, T. J. Wolery, W. Bourcier, A. F. B. Tompson, E. D. Jones, S. J. Friedmann and R. D. Aines (2011). Combining Brine Extraction, Desalination, and Residual-Brine Reinjection with CO2 Storage in Saline Formations: Implications for Pressure Management, Capacity, and Risk Mitigation. 10th International Conference on Greenhouse Gas Control Technologies. J. Gale, C. Hendriks and W. Turkenberg. Amsterdam, Elsevier Science Bv. **4:** 4283-4290.

Dake, L. P. (2001). Practice of Reservoir Engineering (Revised Edition), Elsevier**:** 572.

de Coninck, H. C., L. A. Meyer, B. Metz, O. Davidson and M. M. Loos (2005). "IPCC special report on carbon dioxide capture and storage." Working Group III of the Intergovernmental Panel on Climate Change.

Fard, M. H., K. Hooman and H. T. Chua (2010). "Numerical simulation of a supercritical CO2 geothermosiphon." International Communications in Heat and Mass Transfer **37**(10): 1447-1451.

Haghshenas Fard, M., K. Hooman and H. T. Chua (2010). "Numerical simulation of a supercritical CO2 geothermosiphon." International Communications in Heat and Mass Transfer **37**(10): 1447-1451.

Hameed, S., R. D. Cess and J. S. Hogan (1980). "Response of the global climate to changes in atmospheric chemical composition due to fossil fuel burning." Journal of Geophysical Research **85**(C12): 7537-7545.

Havlena, D. and A. S. Odeh (1963). "The Material Balance as an Equation of a Straight Line." Transactions of the Society of Petroleum Engineers of Aime **228**(8): 896-900.

Jones, G. S., A. Jones, D. L. Roberts, P. A. Stott and K. D. Williams (2005). "Sensitivity of global-scale climate change attribution results to inclusion of fossil fuel black carbon aerosol." Geophysical Research Letters **32**(14): 1-4.

Klise, G. T., J. D. Roach, P. H. Kobos, J. E. Heath and K. A. Gutierrez (2013). "The cost of meeting increased cooling-water demands for CO2 capture and storage utilizing non-traditional waters from geologic saline formations." Hydrogeology Journal **21**(3): 587-604.

Lund, J. W., L. Bjelm, G. Bloomquist and A. K. Mortensen (2008). "Characteristics, development and utilization of geothermal resources - a Nordic perspective." Episodes **31**(1): 140-147.

Magliocco, M., Kneafsey, T., Pruess, K., Glaser, S. (2011). Laboratory experimental study of heat extraction from porous media by means of CO2. Proceedings of the Thirty-sixth Workshop on Geothermal Reservoir Engineering, Stanford University, Stanford, CA.

Majorowicz, J. and S. E. Grasby (2010). "High Potential Regions for Enhanced Geothermal Systems in Canada." Natural resources research (New York, N.Y.) **19**(3): 177-188.

Paulus, M. E. and S. G. Penoncello (2006). "Correlation for the carbon dioxide and water mixture based on the Lemmon-Jacobsen mixture model and the Peng-Robinson equation of state." International Journal of Thermophysics **27**(5): 1373-1386.

Pruess, K. (2006). "Enhanced geothermal systems (EGS) usingCO(2) as working fluid - A novel approach for generating renewable energy with simultaneous sequestration of carbon." Geothermics **35**(4): 351-367.

Pruess, K. (2008). "On production behavior of enhanced geothermal systems with CO2 as working fluid." Energy Conversion and Management **49**(6): 1446-1454.

Rosenbauer, R. J., T. Koksalan and J. L. Palandri (2005). "Experimental investigation of CO2-brine-rock interactions at elevated temperature and pressure: Implications for CO2 sequestration in deep-saline aquifers." Fuel Processing Technology **86**(14-15): 1581-1597.

Span, R. and W. Wagner (1996). "A new equation of state for carbon dioxide covering the fluid region from the triple-point temperature to 1100 K at pressures up to 800 MPa." Journal of Physical and Chemical Reference Data **25**(6): 1509-1596.

Spycher, N. and K. Pruess (2010). "A Phase-Partitioning Model for CO2-Brine Mixtures at Elevated Temperatures and Pressures: Application to CO2-Enhanced Geothermal Systems." Transport in Porous Media **82**(1): 173-196.

Ueda, A., K. Kato, T. Ohsumi, T. Yajima, H. Ito, H. Kaieda, R. Metcalfe and H. Takase (2005). "Experimental studies of CO2-rock interaction at elevated temperatures under hydrothermal conditions." Geochemical Journal **39**(5): 417-425.

Wan, Y., Xu, T., Pruess, K. (2011). Impact of fluid-rock interactions on enhanced geothermal systems with CO2 as heat transmission fluid. Proceedings of the Thirty-sixth Workshop on Geothermal Reservoir Engineering, Stanford University, Stanford, CA.

Xu, T., Pruess, K. (2010). Reactive transport modeling to study fluid–rock interactions in enhanced geothermal systems (EGS) with CO2 as working fluid. Proceedings of World Geothermal Congress 2010, Bali, Indonesia.

Xu, T., Pruess, K., Apps, J. (2008). Numerical studies of fluid–rock interactions in enhanced geothermal systems (EGS) with CO2 as working fluid. Proceedings of the Thirty-third Workshop on Geothermal Reservoir Engineering, Stanford University, Stanford, CA.

Xu, T., Zhang, W., Pruess, K. (2010). Numerical simulation to study feasibility of using CO2 as stimulation agent for enhanced geothermal systems. Proceedings of the Thirty-fifth Workshop on Geothermal Reservoir Engineering, Stanford University, Stanford, CA.

Zimmermann, G., I. Moeck and G. Blocher (2010). "Cyclic waterfrac stimulation to develop an Enhanced Geothermal System (EGS)-Conceptual design and experimental results." Geothermics **39**(1): 59-69.